

Dynamical formation and manipulation of Majorana fermions in driven quantum wires

E. Perfetto

*Dipartimento di Fisica, Università di Roma Tor Vergata,
Via della Ricerca Scientifica 1, I-00133 Rome, Italy*

Controlling the dynamics of Majorana fermions (MF) subject to time-varying driving fields is of fundamental importance for the practical realization of topological quantum computing. In this work we study how it is possible to dynamically generate and maintain the topological phase in one-dimensional superconducting nanowires after the temporal variation of the Hamiltonian parameters. Remarkably we show that for a sudden quench the system can never relax towards a state exhibiting fully developed MF, independently of the initial and final Hamiltonians. Only for sufficiently slow protocols the system behaves adiabatically, and the topological phase can be reached. Finally we address the crucial question of how “adiabatic” a protocol must be in order to manipulate the MF inside the topological phase without deteriorating their Majorana character.

PACS numbers: 74.78.Fk, 73.63.Nm, 74.40.Gh

Introduction.— The enormous potential of Majorana fermions (MF) for implementing decoherence-free quantum computation[1] is greatly stimulating their search in solid state systems. Several different platforms have been proposed for realizing MF, like fractional quantum Hall states at filling factor $5/2$, vortex cores of $p + ip$ superconductors[2], surfaces of topological insulators coupled to s -wave superconductors[3], non-centrosymmetric superconductors[4], and ferromagnetic Josephson junctions[5]. However, despite such intense theoretical activity, no experimental evidence of the existence of MF in the above systems has been provided so far. A promising alternative that should drastically simplify the realization and detection of MF consists in forming one-dimensional (1D) heterostructures with semiconductors and conventional superconductors[6, 7]. Here the p -wave superconductivity is simulated by means of spin-orbit (SO) interaction and the system can be driven into the topological (T) phase (where the MF appear) by applying a suitable magnetic field. In addition MF occurring in 2D and 3D networks of these nanowires are particularly attracting, since they can be adiabatically manipulated by using tunable gates or by reorienting of the magnetic field[7, 8]. Very recently signatures of MF presence in InSb and InAs nanowires have been reported[9–12]. Quantum wires hosting MF could also be engineered in trapped ultracold fermionic atoms, by employing optical Raman transitions to generate effective spin-orbit coupling and Zeeman fields, and using the proximity effect with a bulk molecular Bose-Einstein condensate[13]. In these systems one can tune the parameters with high temporal precision and efficiently control the amount of disorder. Thus they offer a unique possibility to study in a very clean way the nonequilibrium dynamics of MF following time-dependent perturbations, and in particular their formation when the system undergoes the topological phase transition.

In this Letter we study the real-time dynamics of a 1D quantum wire of finite length in contact with a su-

perconductor and in presence of SO coupling. The system is driven out of equilibrium by varying the external magnetic field by means of different protocols. The formation of MF is monitored by calculating the evolution of the recently proposed Majorana order parameter[14]. Remarkably we show that for sudden variations of the Hamiltonian the system relaxes towards a nonthermal state that does not exhibit fully developed MF. Only for sufficiently slow protocols the system undergoes the topological phase transition, over a timescale which increases with increasing length of the wire. Finally we show that the manipulation of MF inside the T phase must obey precise temporal constraints in order to preserve the Majorana character. This is a crucial issue for the practical implementation of topological quantum computing.

Model and formalism.— The Hamiltonian of the coupled wire of length \mathcal{L} is given by[7, 15]

$$H = \int_0^{\mathcal{L}} dx \Psi^\dagger(x) (-\partial_x^2/2m - \mu - i\alpha\partial_x\sigma_y + V_z\sigma_z) \Psi(x) + \Delta(\psi_\uparrow(x)\psi_\downarrow(x) + \text{h.c.}), \quad \Psi^\dagger = (\psi_\uparrow^\dagger, \psi_\downarrow^\dagger), \quad (1)$$

where σ_i are the Pauli matrices, $\psi_\sigma(x)^{(\dagger)}$ annihilates (creates) an electron of mass m and spin σ at position x in the wire, μ is the chemical potential, Δ is the strength of the proximity pairing field, and α and V_z are the amplitudes of SO coupling and Zeeman field respectively. This model displays a topologically trivial (TT) phase for $Q \equiv \mu^2 + \Delta^2 - V_z^2 > 0$ and a T phase for $Q < 0$, the phase transition occurring at $Q = 0$ [6, 7]. The existence of MF in the T phase can be probed by considering the Majorana polarization[14], defined as the anomalous local density of states

$$P(x, \omega) = -\frac{1}{\pi} \text{Im} \int_0^\infty e^{i\omega t} \sum_\sigma 2i \langle \{ \psi_\sigma^\dagger(x, t), \psi_\sigma^\dagger(x, 0) \} \rangle, \quad (2)$$

where the average is taken over the Hamiltonian ground-state $|\Psi_0\rangle$. As discussed in Refs. [14, 16] a good order

parameter to detect the T phase can be built from P as

$$\Phi = \int_0^{\mathcal{L}/2} dx P(x, 0) = - \int_{\mathcal{L}/2}^{\mathcal{L}} dx P(x, 0). \quad (3)$$

Indeed in the TT phase it holds $\Phi = 0$, while in the T phase only the MF contribute to the order parameter yielding $\Phi = 1$. The nonanalytic behavior of Φ at $Q = 0$ indicates the occurrence of the phase transition, while values of Φ close to 1 signal MF not fully developed. It is worth observing that for noninteracting fermions [as in the case of Hamiltonian in Eq. (1)] the polarization takes the simpler form[14]

$$P(x, \omega) = 2 \sum_{n, \sigma} \delta(\omega - \epsilon_n) u_{\sigma}^{(n)*}(x) v_{\sigma}^{(n)}(x), \quad (4)$$

where n denotes the n -th eigenstate of the system with eigenvalue ϵ_n and wavefunction $(u_{\uparrow}^{(n)}, v_{\downarrow}^{(n)}, u_{\downarrow}^{(n)}, v_{\uparrow}^{(n)})$ expressed in the basis $(\psi_{\uparrow}^{\dagger}, \psi_{\downarrow}, \psi_{\downarrow}^{\dagger}, \psi_{\uparrow})$.

The pair of (real) zero-energy MF supported by the Hamiltonian H in the T phase are located at the two opposite edges of the wire[6, 7] and decay exponentially into the bulk. The corresponding wavefunction must obey the constraint $u_{\sigma} = v_{\sigma}$ (that ensures the particle/antiparticle equivalence) and can be found by solving the auxiliary problem[6]

$$\begin{pmatrix} -\partial_x^2/2m - \mu + V_z & -\eta\Delta + \alpha\partial_x \\ \eta\Delta - \alpha\partial_x & -\partial_x^2/2m - \mu - V_z \end{pmatrix} \begin{pmatrix} u_{\uparrow}(x) \\ u_{\downarrow}(x) \end{pmatrix} = 0, \quad (5)$$

where $\eta = \pm 1$. The two choices of η provide the MF located at the right and left boundary of the wire respectively. In the following we assume $\eta = 1$, since the calculation with $\eta = -1$ follows the same line of reasoning. The MF wavefunction is then obtained by imposing the ansatz

$$\begin{pmatrix} u_{\uparrow}(x) \\ u_{\downarrow}(x) \end{pmatrix} = \begin{pmatrix} U_{\uparrow} \\ U_{\downarrow} \end{pmatrix} g(x), \quad (6)$$

with $g(x) = e^{-x/\ell}$ [17]. The characteristic equation for ℓ has in principle 4 complex solutions for a given l . However, in the T phase (i.e. for $Q < 0$) and for any $\eta = \pm 1$ only a single solution is real and ensures the normalizability of the wavefunction[6]. In addition it is straightforward to verify that the allowed ℓ for $\eta = \pm 1$ do coincide, as dictated by symmetry constraints. The coefficients U_{σ} are easily obtained and read

$$\begin{aligned} U_{\uparrow} &= \frac{\ell^{-1/2}}{\sqrt{1 + \left(\frac{V_z - \frac{\ell-2}{2m} - \mu}{\alpha/\ell + \Delta} \right)^2}}, \\ U_{\downarrow} &= \frac{\ell^{-1/2}}{\sqrt{1 + \left(\frac{\alpha/\ell + \Delta}{V_z - \frac{\ell-2}{2m} - \mu} \right)^2}}. \end{aligned} \quad (7)$$

From the above solution we obtain that the Majorana order parameter $\Phi = 2\eta\ell \sum_{\sigma} U_{\sigma}^2$ is 1 in the left half-wire and -1 in the right half-wire, as it should be[16].

Real-time evolution.— We now study the real-time evolution of Φ after the variation of the external magnetic field V_z according to different protocols. The explicit calculations are performed within the tight-binding version of the Hamiltonian in Eq. (1), which reads

$$\begin{aligned} H &= \sum_{i=1}^{\mathcal{N}} -\frac{v}{2} [C_i^{\dagger} C_{i+1} + \text{h.c.} - (\mu - v) C_i^{\dagger} C_i] \\ &- \frac{\alpha}{2} (i C_i^{\dagger} \sigma_y C_{i+1} + \text{h.c.}) + V_z C_i^{\dagger} \sigma_z C_i \\ &+ \Delta (c_{i\uparrow} c_{i\downarrow} + \text{h.c.}), \quad C_i^{\dagger} = (c_{i\uparrow}^{\dagger}, c_{i\downarrow}^{\dagger}), \end{aligned} \quad (8)$$

with $\mathcal{N} = \mathcal{L}/a$ and a the lattice spacing. The mapping between the parameters of the continuum and lattice models is discussed in Ref. [18]. In the following we express energies in units of the hopping v and times in units of $1/v$. If $V_z \rightarrow V_z(t)$ the Hamiltonian becomes explicitly time-dependent $H \rightarrow H(t)$ and the dynamics of the system is addressed by propagating the equilibrium ground-state $|\Psi_0\rangle$ appearing in Eq. (2) according to $|\Psi_0(t)\rangle = \mathcal{T} \exp[-i \int_0^t ds H(s)] |\Psi_0\rangle$, where \mathcal{T} is the time-ordering operator. The problem is numerically solved by discretizing the time and calculating the evolution of $|\Psi_0\rangle$ within a time-stepping procedure $|\Psi_0(t_j)\rangle \approx \exp[-i H(t_j) \delta t] |\Psi_0(t_{j-1})\rangle$, where $t_j = j \delta t$, δt being a small time step and j a positive integer[19, 20]. We have considered ramp-like switching protocols of duration τ bringing the magnetic field from the initial value $V_z^{(i)}$ at $t = 0$ [with corresponding Hamiltonian $H(0) \equiv H_i$] to the final value $V_z^{(f)}$ [with Hamiltonian $H(t > \tau) \equiv H_f$] which is maintained constant for $t > \tau$, i.e. $V_z(t) = \theta(\tau - t)[V_z^{(i)} + (V_z^{(f)} - V_z^{(i)})t/\tau] + \theta(t - \tau)V_z^{(f)}$. The order parameter is then extracted by following Ref. [14]. Since energy is not conserved during the temporal evolution, we calculate $\Phi(t)$ by integrating over x the instantaneous polarization $P(x, E_{\text{opt}}(t))$, where $E_{\text{opt}}(t)$ is the minimum average of $H(t)$ over the evolved eigenstates of H_i , denoted by $|\phi_n(t)\rangle$ [21]. At every time the states corresponding to the minimum energy are always two, with same value of $|E_{\text{opt}}(t)|$, but with opposite signs due to the symmetry of the problem. Therefore the two optimal $|\phi_{\text{opt}}(t)\rangle$ [with wavefunctions $u_{\sigma}^{(\text{opt})}(x, t), v_{\sigma}^{(\text{opt})}(x, t)$ to be inserted in Eq. (4)] are the best approximation to the pair of MF that the system can provide at a given time.

Quench dynamics.— If $\tau = 0^+$ we have a so-called sudden quench. We have studied two relevant situations, namely (i) the system initially in the TT phase and the value $V_z^{(f)}$ such that $Q < 0$ for the final Hamiltonian (TT \rightarrow T quench), and (ii) $Q < 0$ both for the initial and final systems (T \rightarrow T quench). The first case serves to understand how the MF are dynamically formed, while

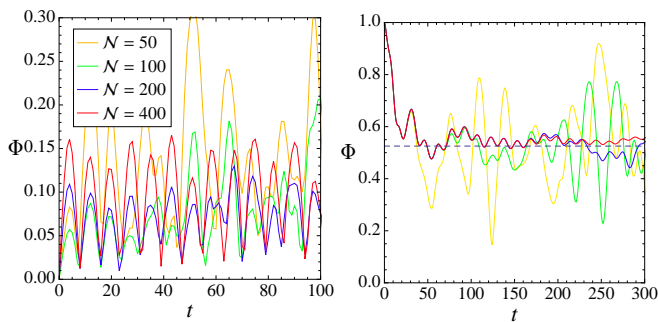


FIG. 1: Φ as a function of time for a $TT \rightarrow T$ quench with $V_z^{(i)} = 10^{-6}$ and $V_z^{(f)} = 0.2$ (left panel), and for a $T \rightarrow T$ quench with $V_z^{(i)} = 0.2$ and $V_z^{(f)} = 0.3$ (right panel). The rest of parameters are $\mu = 0$, $\Delta = 0.1$, $\alpha = 0.3$. The dashed line in the right panel represents Φ_{GGE} calculated as in Eq. (10). Φ_{GGE} has been obtained with $\mathcal{N} = 400$, but its value depends very weakly on \mathcal{N} .

the second case is crucial to investigate whether the MF maintain their character after a manipulation of the system parameters *inside* the T phase. In Fig. 1 we show the time evolution of the order parameter in the two cases, for different values of the size \mathcal{N} . Remarkably *if the system is initially in the TT phase the MF do not form* after the quench, and the order parameter remains close to zero for any \mathcal{N} , displaying temporal oscillations due to the finite size of the system (Fig. 1 left panel). If instead the system is initially in the T phase, we see that the MF of H_i are corrupted by the quench dynamics even if the condition $Q < 0$ is maintained at all times, and Φ approaches finite values significantly smaller than 1 (Fig. 1 right panel). Also in this case $\Phi(t)$ displays oscillations which, however, tend to disappear by increasing \mathcal{N} . We have verified that similar results are also found by quenching other quantities like the strength of the pairing field, the SO coupling or the chemical potential (not show). The above findings indicate that after a sudden quench the initial ground-state $|\Psi_0\rangle$ does not relax to the ground-state of the quenched Hamiltonian[22–25], and, more in important, that no single-particle eigenstate of H_i transforms into the MF of H_f . It has been conjectured[26] that some of the properties of the non-thermal state that develops after a sudden quench can be addressed within the so-called generalized Gibbs ensemble (GGE). The GGE permits to compute a class of long-time averages of of integrable quenched systems by means of the special density matrix[26]

$$\rho_{\text{GGE}} = \frac{1}{Z_{\text{GGE}}} e^{-\sum_n \lambda_n \mathcal{I}_n}, \quad (9)$$

where $Z_{\text{GGE}} = \text{Tr}[e^{-\sum_n \lambda_n \mathcal{I}_n}]$ and \mathcal{I}_n are a set of integrals of motion of the quenched Hamiltonian. The weights λ_n are fixed by the condition $\text{Tr}[\rho_{\text{GGE}} \mathcal{I}_n] = \langle \mathcal{I}_n \rangle_{t=0}$. Thus one can argue that the average of an

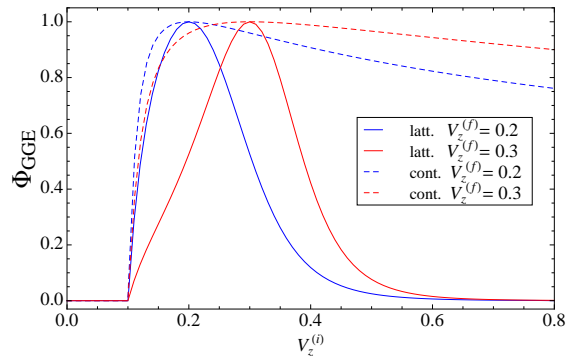


FIG. 2: Φ_{GGE} for a $T \rightarrow T$ quench as a function of $V_z^{(i)}$ at fixed $V_z^{(f)} = 0.2$ and $V_z^{(f)} = 0.3$ for both the continuum and the lattice models. The rest of parameters are the same as in Fig. 1. We set $a = 1$ and hence $m = 1/v$ [18]. For the lattice model we computed numerically Eq. (10) by diagonalizing H with $\mathcal{N} = 200$ (the result is however quite insensitive on the value of \mathcal{N}) while for the continuum model we used the analytic wavefunction in Eqs. (6,7).

observable O after the quench is obtained as $O_{\text{GGE}} = \text{Tr}[\rho_{\text{GGE}} O]$. In the present case we choose \mathcal{I}_n as the eigenmode-occupations of the quenched Hamiltonian, i.e. $\mathcal{I}_n = \gamma_n^\dagger \gamma_n$ where $H_f = \sum_n \epsilon_n \gamma_n^\dagger \gamma_n$. As long as only the zero-energy states contribute to Φ , the GGE is, in this case, spanned by the pair of MF. Thus the order parameter calculated within the GGE takes an elegant analytic expression, being given by the square modulus of the overlap between the (real) MF of the initial Hamiltonian and those of the final Hamiltonian

$$\Phi_{\text{GGE}} = \left| \sum_{\sigma} \int_0^{\mathcal{L}/2} dx u_{\sigma}^{(i)}(x) u_{\sigma}^{(f)}(x) \right|^2, \quad (10)$$

where i and f denote the MF wavefunctions calculated with respect to H_i and H_f respectively. As shown in Fig. 1 the long-time average of Φ after the sudden quench is in very good agreement with the corresponding quantity calculated within the GGE. For the $TT \rightarrow T$ quench the GGE predicts $\Phi_{\text{GGE}} = 0$ since H_i has no MF; accordingly the real-time simulations provide values of $\Phi(t)$ close to 0, see left panel Fig. 1. In the case of the $T \rightarrow T$ quench the agreement is even more remarkable, see dashed line in right panel. Indeed the oscillations of $\Phi(t)$ (sizable only for $\mathcal{N} \lesssim 100$) are exactly centered around the value Φ_{GGE} . Thus we can infer that the GGE provides accurate predictions of the asymptotic quench dynamics of the Majorana order parameter.

In Fig. 2 we illustrate the robustness of the T phase after a $T \rightarrow T$ quench. The value Φ_{GGE} is plotted as a function of the strength of the initial magnetic field $V_z^{(i)}$, for a fixed value of the target $V_z^{(f)}$. We see that if $\Delta < V_z^{(i)} < V_z^{(f)}$ the T phase is readily corrupted, even for small differences between the strengths of the initial and final magnetic fields. This happens in both the con-

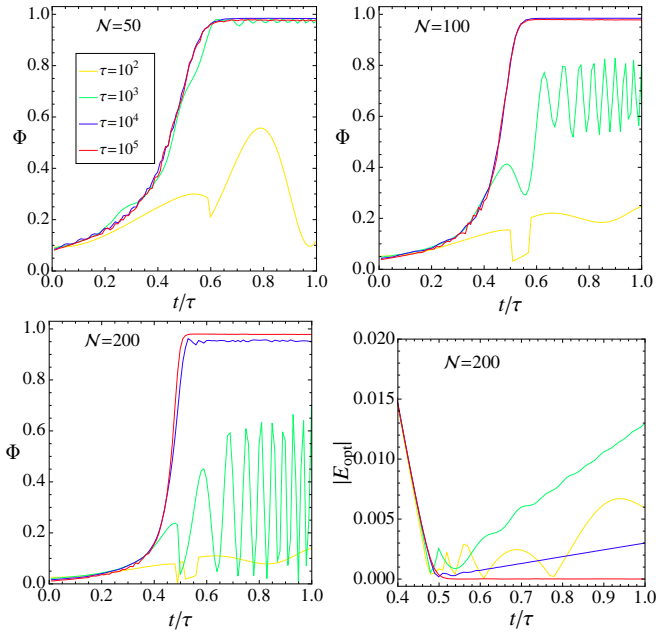


FIG. 3: Φ and lowest energy E_{opt} as a function of time for $\text{TT} \rightarrow \text{T}$ transitions with different ramp duration and wire length. The protocol parameters are $V_z^{(i)} = 0.01$ and $V_z^{(f)} = 0.3$ and the rest of parameters are the same as in Fig. 1. The discontinuities in $\Phi(t)$ observed for $\tau = 10^2$ are due to dynamical level crossings in the set $\{\varepsilon_n(t)\}$ [21].

tinuum and in the lattice models. If $V_z^{(i)} > V_z^{(f)}$, instead, the continuum model predicts a significantly more stable T phase, since the system can afford larger changes in V_z still maintaining values of Φ close to 1 (see Fig. 2 dashed lines).

Ramp protocols.— We now investigate the possibility of generating/maintaining the T phase after an arbitrary change in the strength of the magnetic field by considering ramp protocols of finite duration τ . In Fig. 3 we plot $\Phi(t)$ for different $\text{TT} \rightarrow \text{T}$ transitions by varying τ and \mathcal{N} . It is seen that for sufficiently slow ramps the topological phase transition takes place and MF fully develop, in agreement with the adiabatic hypothesis. We mention, however, that the validity of the adiabatic theorem is not obvious in the present context, since the final Hamiltonian is such that its square H_f^2 has a doubly degenerate ground-state, i.e. the pair of MF [27]. In the lower-right panel we also plot $E_{\text{opt}}(t)$. For $\mathcal{N} = 200$ and $\tau = 10^5$ the formation of the MF is clearly visible as E_{opt} approaches zero when $V_z(t)$ overcomes Δ (i.e. when Q becomes negative). Still, our results clearly indicate that the duration τ required to reach $\Phi = 1$ increases with increasing size. For instance $\tau \sim 10^3$ is required to create MF in a wire of length $\mathcal{N} = 50$, whereas τ increases of about two orders of magnitude by enlarging the system to $\mathcal{N} = 200$. Interestingly this trend is reversed if one considers $\text{T} \rightarrow \text{T}$ transitions. In this case the larger is the size of the wire, the shorter is the ramp-time needed

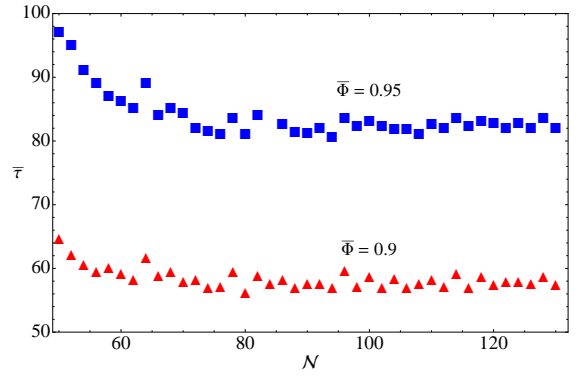


FIG. 4: Ramp-duration $\bar{\tau}$ required for a $\text{T} \rightarrow \text{T}$ transition to reach the asymptotic value $\bar{\Phi} = 0.95$ (boxes) and $\bar{\Phi} = 0.9$ (triangles) as a function of the length \mathcal{N} . The protocol parameters are $V_z^{(i)} = 0.2$ and $V_z^{(f)} = 0.3$, and the rest of parameters are the same as in Fig. 1.

to maintain the Majorana character after the transformation. In Fig. 4 we show the duration $\bar{\tau}$ required for $\text{T} \rightarrow \text{T}$ transition to reach a desired value $\bar{\Phi}$ of the order parameter (averaged over long times) close to 1. It appears that $\bar{\tau}$ is an overall decreasing function of \mathcal{N} (although with relatively small oscillations) that for the chosen parameters saturates to the finite value $\bar{\tau} \approx 80$ for $\bar{\Phi} = 0.95$ and $\bar{\tau} \approx 60$ for $\bar{\Phi} = 0.9$. We have checked (not shown) that this qualitative behavior does not change by varying the features of the protocol, thus providing an explicit measure of adiabaticity for protocols aiming at preserving MF.

Conclusions.— We have studied the temporal evolution of MF in driven 1D quantum wires after the variation of the system parameters according to different protocols. In the case of sudden quenches, thermalization breakdown is observed, and the long-time behavior of the Majorana order parameter Φ is well described within the GGE. Remarkably we find that the relaxed state does not display fully developed MF, no matter the initial Hamiltonian is: for a $\text{TT} \rightarrow \text{T}$ quench the MF are not generated and Φ remains close to zero, while for a $\text{T} \rightarrow \text{T}$ quench the MF initially present get readily corrupted as the system is driven out of equilibrium. The adiabatic theorem is, instead, recovered for extremely slow ramp protocols. In the case of a slow $\text{TT} \rightarrow \text{T}$ ramp the system undergoes dynamically the topological phase transition within a timescale that increases by increasing the length of the wire. Finally we have provided an explicit estimate of adiabaticity to preserve MF during $\text{T} \rightarrow \text{T}$ protocols, by pointing out the existence of precise temporal constraints relevant for the topological quantum computation.

- [2] D. A. Ivanov, Phys. Rev. Lett. **86**, 268 (2001).
- [3] L. Fu and C. L. Kane, Phys. Rev. Lett. **100**, 096407 (2008).
- [4] M. Sato, Y. Takahashi, and S. Fujimoto, Phys. Rev. Lett. **103**, 020401 (2009).
- [5] A. M. Black-Schaffer, and J. Linder, Phys. Rev. B **84**, 180509(R) (2011).
- [6] R. M. Lutchyn, J. D. Sau and S. Das Sarma, Phys. Rev. Lett. **105**, 077001 (2010).
- [7] Y. Oreg, G. Refael and F. von Oppen, Phys. Rev. Lett. **105**, 177002 (2010).
- [8] J. Alicea, Y. Oreg, G. Refael, F. von Oppen, and M. P. A. Fisher, Nature Phys. **7**, 412 (2011).
- [9] V. Mourik, K. Zuo, S.M. Frolov, S.R. Plissard, E. P. A. M. Bakkers, and L.P. Kouwenhoven, Science **336**, 1003 (2012).
- [10] L. Rokhinson, X. Liu, and J. Furdyna, arXiv:1204.4212.
- [11] A. Das, Y. Ronen, Y. Most, Y. Oreg, M. Heiblum, and H. Shtrikman, arXiv:1205.7073.
- [12] M. T. Deng, C. L. Yu, G. Y. Huang, M. Larsson, P. Caroff, and H. Q. Xu, arXiv:1204.4130.
- [13] L. Jiang, T. Kitagawa, J. Alicea, A. R. Akhmerov, D. Pekker, G. Refael, J. I. Cirac, E. Demler, M. D. Lukin, and P. Zoller, Phys. Rev. Lett. **106**, 220402 (2011).
- [14] D. Sticlet, C. Bena, and P. Simon, Phys. Rev. Lett. **108**, 096802 (2012).
- [15] Through this paper we use $\hbar = e = 1$.
- [16] D. Chevallier, D. Sticlet, P. Simon, and C. Bena, Phys. Rev. B **85**, 235307 (2012).
- [17] We assume that $\mathcal{L} \gg \ell$ in order to calculate independently the MBs at the two edges, and also to simplify their normalization condition.
- [18] E. M. Stoudenmire, J. Alicea, O. A. Starykh, and M. P. A. Fisher, Phys. Rev. B **84**, 014503 (2011).
- [19] E. Perfetto, G. Stefanucci, and M. Cini, Phys. Rev. B **80**, 205408 (2009).
- [20] G. Stefanucci, E. Perfetto, and M. Cini, Phys. Rev. B **81**, 115446 (2010).
- [21] In other words $E_{\text{opt}}(t) = \min\{|\varepsilon_n(t)|\}$, with $\varepsilon_n(t) = \langle \phi_n(t) | H(t) | \phi_n(t) \rangle$.
- [22] M. A. Cazalilla, Phys. Rev. Lett. **97**, 156403 (2006).
- [23] A. Iucci and M. A. Cazalilla, Phys. Rev. A **80**, 063619 (2009).
- [24] E. Perfetto, Phys. Rev. B. **74**, 205123 (2006).
- [25] E. Perfetto and G. Stefanucci, EPL **95**, 10006 (2011).
- [26] M Rigol, V. Dunjko, V. Yurovsky, and M. Olshanii, Phys. Rev. Lett. **98**, 050405 (2007).
- [27] A. Messiah, Quantum Mechanics, North-Holland Pub. Co., (1962).